

External Heavy-Atom Effect on the Prompt and Delayed Fluorescence of [70]Fullerenes

Carlos Baleizão and Mário N. Berberan-Santos^{*[a]}

The influence of the external heavy-atom effect (HAE) on the fluorescence properties of C_{70} and a C_{70} methano monoadduct is determined. For this purpose the photophysics of these [70]fullerenes is studied in polystyrene (PS) and in a related heavy-atom polymer, poly(4-bromostyrene) (PBS). In the absence of HAE (PS matrix) both fullerenes display a strong thermally activated delayed fluorescence (DF) that is more pronounced in the case of C_{70} . In the presence of HAE (PBS matrix) both prompt (PF) and DF intensities decrease significantly, the same happening to the delayed fluorescence lifetimes. The relative fluorescence intensities (DF intensity/PF in-

tensity) for each fullerene are on the other hand surprisingly similar to the respective ones in PS for the full experimental temperature range. The HAE is responsible for a significant increase of the $S_1 \rightarrow T_1$ and $S_1 \leftarrow T_1$ intersystem crossing (ISC) rates, and of the $T_1 \rightarrow S_0$ radiative rate. In particular, the HAE on a $S_1 \leftarrow T_1$ ISC rate is reported here for the first time. The overall substantial insensitivity of relative fluorescence intensities to HAE is explained by a compensation effect: As the $S_1 \rightarrow T_1$ and $S_1 \leftarrow T_1$ ISC rates on the one hand, and the $T_1 \rightarrow S_0$ radiative rate on the other hand work in opposition with respect to DF, a near cancellation of effects occurs.

1. Introduction

Molecular fluorescence can take place by two different unimolecular mechanisms: prompt fluorescence (PF) and thermally activated delayed fluorescence (DF).^[1] In the PF mechanism, which is by far the most common, emission occurs after $S_n \leftarrow S_0$ absorption and excited-state relaxation to S_1 . On the other hand, DF occurs via the triplet manifold: after excitation and once attained S_1 , intersystem crossing (ISC) to the triplet manifold (triplet state T_1) takes place, followed by a second intersystem crossing back to S_1 , and by fluorescence emission proper. It was recently shown that the cycle $S_1 \rightarrow T_1 \rightarrow S_1$ may repeat a number of times before fluorescence emission is observed.^[2,3] In the case of C_{70} , and for sufficiently high temperatures, the average number of cycles may be as high as 100. DF is significant only when the quantum yield of triplet formation (Φ_T) and the quantum yield of singlet formation (Φ_S) are both high.^[4] This in turn implies a small energy gap between S_1 and T_1 (ΔE_{ST}), a long T_1 lifetime, and not too low a temperature.^[4] Although known for a long time, DF remains an uncommon and usually very weak phenomenon.

The unique photophysical properties of C_{70} , specifically the Φ_T close to one,^[2,4] the small ΔE_{ST} gap^[2,4] and the long intrinsic phosphorescence lifetime,^[2,4] give rise to an exceptionally strong DF for this fullerene.^[2,4] C_{70} derivatives,^[2,5] fullerene C_{60} ^[6] and some C_{60} derivatives^[7,8] also exhibit DF, but it is in all cases weaker than in C_{70} . Recently, and owing to its special DF properties, C_{70} was used as a sensitive probe for both temperature^[9,10] and molecular oxygen.^[11,12]

The fluorescence quenching by heavy atoms (atoms of large atomic number), namely iodide ions and xenon atoms, or heavy-atom bearing compounds like bromobenzene, is named the external heavy-atom effect (HAE).^[1,13] It operates by increasing the $S_1 \rightarrow T_n$ intersystem crossing owing to induced

spin-orbit coupling, a short-range process requiring fluorophore-quencher wavefunction mixing.^[13] It is known that the HAE manifests itself mainly by an increase of the $S_1 \rightarrow T_n$ ISC rate constant and of the $T_1 \rightarrow S_0$ radiative rate constant, the $T_1 \rightarrow S_0$ nonradiative (ISC) rate constant being little affected.^[13] It is expected that the $S_1 \leftarrow T_1$ ISC rate constant will also suffer an increase owing to the HAE, but no results for this are available. Fullerenes with their strong DF offer an excellent opportunity for the study of this effect.

In the case of fullerene C_{60} , phosphorescence above a few kelvin could be observed in an ethyl iodide containing solvent (at 77 K) thanks to the increase of the $T_1 \rightarrow S_0$ radiative rate constant by the HAE.^[14] Quenching of the prompt fluorescence of fullerenes by the HAE has been the subject of several studies.^[15-18] It was established that, in spite of a very efficient intrinsic intersystem crossing (the intrinsic quantum yields of triplet formation being close to 1), fullerenes are still subject to the HAE that may significantly increase the intersystem crossing rate constant. For instance, while the fluorescence lifetime of a C_{70} pseudo-dihydro monoadduct in cyclohexane is 1.1 ns, in bromobenzene it drops to 400 ps, and in methyl iodide it is only 70 ps.^[15] In the case of C_{70} and of the mentioned monoadduct, it was concluded that the quenching was dynamic for

[a] Dr. C. Baleizão, Prof. Dr. M. N. Berberan-Santos
CQFM-Centro de Química-Física Molecular
and IN-Institute of Nanoscience and Nanotechnology
Instituto Superior Técnico, Universidade Técnica de Lisboa
Av. Rovisco Pais, 1049-001 Lisboa (Portugal)
Fax: (351) 218-464-455
E-mail: berberan@ist.utl.pt

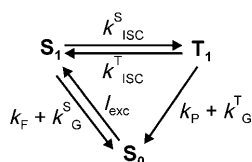
Supporting information for this article is available on the WWW under <http://dx.doi.org/10.1002/cphc.201000395>.

several brominated and iodinated neutral quenchers. The Stern–Volmer plots obtained in hydrocarbon-quencher mixtures smoothly extrapolate to the results in pure liquid quencher solution, for example, bromobenzene.^[15] The quenching was in all cases below diffusion control, and for this reason (weak) fullerene fluorescence was still detected even in pure iodinated quenchers like iodobenzene. The effect was, as expected, stronger in iodinated quenchers than in brominated ones. A detailed study^[17] of the HAE in the case of C₇₀ and two different quenchers, iodide and bromobenzene, provided evidence for a quenching mechanism with exponential distance dependence. It was later shown that the recovered parameters for this mechanism (effective Bohr radius, quenching rate constant at contact) are dependent on the radial distribution used for the quenchers.^[19] In the case of C₆₀ derivatives, including a water-soluble dendrimer,^[16] a quenching effect similar to that for C₇₀ and derivatives was observed for brominated and iodinated quenchers. More recently, the intramolecular and intermolecular HAE on the fluorescence of brominated mono-methano[60]fullerene malonate derivatives was studied. It was observed that the intramolecular effect doubles when going from the dyad to the triad and, when heavy-atoms are present in the solvent (bromobenzene or iodobenzene), the intermolecular effect is predominant.^[18]

In this work, we study for the first time the external heavy-atom effect on the DF, specifically for two [70]fullerenes, pristine C₇₀ and a methano derivative, both dispersed in the heavy-atom containing polymer poly(4-bromostyrene) (PBS). The heavy-atom effect on the S₁←T₁ ISC process is also observed for the first time.

2. Results and Discussion

2.1. DF Kinetics and Data Analysis



Scheme 1. Simplified kinetic scheme for DF.

The simplest model for DF in the condensed phases is a three-state system that can be represented by Scheme 1, where I_{exc} is the excitation intensity, k_{F} and k_{P} are the radiative rate constants for fluorescence and phosphorescence, respectively, k_{G}^{S} and k_{G}^{T} are the nonradiative rate constants for deactivation to the ground state (internal conversion from S₁ and intersystem crossing from T₁, respectively), and $k_{\text{ISC}}^{\text{S}}$ and $k_{\text{ISC}}^{\text{T}}$ are the intersystem crossing rate constants for singlet-to-triplet and triplet-to-singlet conversion, respectively. Owing to the relative energies of S₁ and T₁, the triplet-to-singlet ISC rate constant always corresponds to an activated process that is strongly temperature dependent [Eq. (1)]:^[2,4,13]

$$k_{\text{ISC}}^{\text{T}} = A \exp\left(-\frac{\Delta E_{\text{ST}}}{RT}\right) \quad (1)$$

For strong DF to occur, the following inequalities need to be met: $k_{\text{ISC}}^{\text{S}} \gg k_{\text{F}} + k_{\text{G}}^{\text{S}}$ and $k_{\text{ISC}}^{\text{T}} \gg k_{\text{P}} + k_{\text{G}}^{\text{T}}$. In most cases it is also observed that $k_{\text{ISC}}^{\text{S}} \gg k_{\text{ISC}}^{\text{T}}$ and that $k_{\text{G}}^{\text{S}} \gg k_{\text{P}}$.

The time-evolution of the S₁ and T₁ populations is given by Equations (2) and (3),^[2] where for simplicity the square brackets representing the concentrations are omitted:

$$S_1(t) = \frac{S_1(0)}{\lambda_2 - \lambda_1} [(\lambda_2 - X) \exp(-\lambda_1 t) + (X - \lambda_1) \exp(-\lambda_2 t)] \quad (2)$$

$$T_1(t) = \frac{k_{\text{ISC}}^{\text{S}} S_1(0)}{\lambda_2 - \lambda_1} [\exp(-\lambda_1 t) - \exp(-\lambda_2 t)] \quad (3)$$

where [Eq. (4)]:

$$\lambda_{1,2} = \frac{1}{2} \left\{ X + Y \mp \sqrt{(Y - X)^2 + 4k_{\text{ISC}}^{\text{S}} k_{\text{ISC}}^{\text{T}}} \right\} \quad (4)$$

with [Eqs. (5) and (6)]:

$$\lambda_{1,2} = \frac{1}{2} \left\{ X + Y \mp \sqrt{(Y - X)^2 + 4k_{\text{ISC}}^{\text{S}} k_{\text{ISC}}^{\text{T}}} \right\} \quad (5)$$

$$Y = \frac{1}{\tau_{\text{P}}^0} + k_{\text{ISC}}^{\text{T}} \quad (6)$$

where $\tau_{\text{F}} = 1/(k_{\text{F}} + k_{\text{G}}^{\text{S}} + k_{\text{ISC}}^{\text{S}})$ is the (prompt) fluorescence lifetime. τ_{P}^0 is a hypothetical phosphorescence lifetime in the absence of back ISC, $\tau_{\text{P}}^0 = 1/(k_{\text{P}} + k_{\text{G}}^{\text{T}})$. For rigid molecules, the temperature dependence of k_{G}^{T} is mainly dictated by external effects, such as, interactions with the solvent and other solutes present, for example, oxygen and impurities, and therefore k_{G}^{T} usually changes moderately with temperature in a deoxygenated and photochemically inert solid medium.^[20] In this way, and as the measurements are carried out at higher temperatures (where DF is significant), τ_{P}^0 is expected to be somewhat smaller than the low temperature phosphorescence lifetime.

When inter-conversion between the singlet and triplet emissive states occurs many times before photon emission or non-radiative decay can take place, a fast pre-equilibrium between S₁ and T₁ is established, and for sufficiently long times both S₁ and T₁ decay with a common rate constant given by Equation (7):^[2]

$$\frac{1}{\tau_{\text{DF}}} = \frac{1}{\tau_{\text{P}}^0} + k_{\text{ISC}}^{\text{T}} (1 - \Phi_{\text{T}}) \quad (7)$$

where Φ_{T} is the quantum yield of triplet formation, $\Phi_{\text{T}} = k_{\text{ISC}}^{\text{S}} / (k_{\text{F}} + k_{\text{G}}^{\text{S}} + k_{\text{ISC}}^{\text{S}})$, and τ_{DF} is the delayed fluorescence (and phosphorescence) lifetime.

Using Equation (1), Equation (7) becomes Equation (8):

$$\frac{1}{\tau_{\text{DF}}} = \frac{1}{\tau_{\text{P}}^0} + B \exp\left(-\frac{\Delta E_{\text{ST}}}{RT}\right) \quad (8)$$

where $B = (1 - \Phi_{\text{T}})A$. From a nonlinear fit to the temperature dependence of the fluorescence long component (delayed

fluorescence lifetime) using Equation (8), and assuming that τ_p^0 is temperature independent within the experimental range, it is possible to recover ΔE_{ST} , B and τ_p^0 from time-resolved measurements. Nevertheless, and owing to parameter correlation, it is preferable to fix ΔE_{ST} at the steady-state value [obtained from Eqs. (16) or (18) below]. In this way, A and τ_p^0 can be extracted from the temperature dependence of the delayed fluorescence lifetime.^[2]

The fluorescence quantum yield is given by Equation (9):

$$\Phi_F = \Phi_{PF} + \Phi_{DF} \quad (9)$$

where the quantum yields for prompt Φ_{PF} and delayed Φ_{DF} fluorescence obey Equation (10):^[4]

$$\frac{\Phi_{DF}}{\Phi_{PF}} = \frac{I_{DF}}{I_{PF}} = \frac{1}{\frac{1}{\Phi_T} - 1} \quad (10)$$

and the quantum yield of singlet formation is defined by Equation (11):

$$\Phi_S = \frac{k_{ISC}^T}{k_p + k_G^T + k_{ISC}^T} \quad (11)$$

For strong DF to occur the cycle $S_1 \rightarrow T_1 \rightarrow S_1$ must repeat a number of times before photon emission or nonradiative decay can take place. The average number of cycles \bar{n} is given by Equation (12):

$$\bar{n} = \frac{1}{\frac{1}{\Phi_T} - 1} = \frac{1}{\frac{1}{\Phi_T} \left(1 + \frac{1}{k_{ISC}^T \tau_p^0}\right) - 1} \quad (12)$$

Comparison of Equations (10) and (12) gives Equation (13):

$$\frac{\Phi_{DF}}{\Phi_{PF}} = \frac{I_{DF}}{I_{PF}} = \bar{n} \quad (13)$$

and, using Equation (9), Equation (14) is derived:

$$\frac{\Phi_F}{\Phi_{PF}} = \frac{I_F}{I_{PF}} = 1 + \bar{n} \quad (14)$$

hence the increase in fluorescence intensity owing to DF is a direct measure of the average number of $S_1 \rightarrow T_1 \rightarrow S_1$ cycles performed.^[2,3]

In the absence of reversibility, $\bar{n} = 0$. On the other hand, for the fastest possible excited state equilibration ($k_{ISC}^T \rightarrow A$, $\Phi_S \approx 1$) Equation (15) is adhered to:

$$\bar{n}_{\max} \approx \frac{1}{\frac{1}{\Phi_T} - 1} \quad (15)$$

Several methods of DF intensity data analysis exist. The classic one, due to Parker,^[21] combines steady-state delayed fluorescence and phosphorescence intensities for the determination of ΔE_{ST} . This method was successfully applied to C_{70} .^[4] Nevertheless, in many cases it is not possible or convenient to

measure the phosphorescence, and it is precisely in these cases that a non-spectroscopic method for the estimation of ΔE_{ST} becomes valuable. Furthermore, photophysical parameters other than ΔE_{ST} are of interest and can be extracted from experimental DF data by other methods.

For the purpose of curve fitting, Equation (14) can be conveniently rewritten as Equation (16):^[4]

$$\ln \left[\frac{I_{PF}}{I_{DF}} - \left(\frac{1}{\Phi_T} - 1 \right) \right] = \ln \left[\frac{1}{\Phi_T} \left(\frac{1}{\Phi_S^\infty} - 1 \right) \right] + \frac{\Delta E_{ST}}{RT} \quad (16)$$

where [Eq. (17)]:

$$\Phi_S^\infty = \frac{1}{1 + \frac{1}{A\tau_p^0}} \quad (17)$$

and from a fit to steady-state data arranged in the above form it is possible to recover not only ΔE_{ST} but also Φ_T and Φ_S^∞ , assuming that Φ_S^∞ is temperature independent. Alternatively, a non-linear curve fitting can also be carried out giving Equation (18):

$$\frac{I_{DF}}{I_{PF}} = (a + be^{c/T})^{-1} \quad (18)$$

where [Eqs. (19)–(21)]:

$$a = \frac{1}{\Phi_T} - 1 \quad (19)$$

$$b = \frac{1}{\Phi_T} \left(\frac{1}{\Phi_S^\infty} - 1 \right) \quad (20)$$

$$c = \frac{\Delta E_{ST}}{R} \quad (21)$$

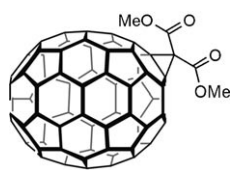
A third method of analysis combines steady-state and time-resolved DF data in a linear plot [Eq. (22)]:^[2]

$$\tau_{DF} = \tau_p^0 - \left(\frac{1}{\Phi_T} - 1 \right) \tau_p^0 \frac{I_{DF}}{I_{PF}} \quad (22)$$

The linear regression according to Equation (22) yields Φ_T and τ_p^0 , again assuming τ_p^0 to be constant within the experimental temperature range, which can be checked by the absence of curvature.

In conclusion, from steady-state and time-resolved fluorescence, it is possible to obtain Φ_T , τ_p^0 , A , and ΔE_{ST} by a plethora of methods. The data analysis methodology followed in this work consists in the use of Equations (16) (or 18) and (22): Equation (16) yields ΔE_{ST} , Φ_T and Φ_S^∞ , and Equation (22) yields Φ_T and τ_p^0 . This offers a consistency check for Φ_T . Finally, parameter A is obtained from Φ_S^∞ and τ_p^0 according to Equation (17).

2.2. Absorption and Prompt Fluorescence



Scheme 2. Chemical structure of C_{70} derivative **1**.

To evaluate the effect of the HAE on a C_{70} derivative, we synthesized a methano adduct, **1** (Scheme 2), using a modified Bingel procedure as described in the Supporting Information.

The fluorescence of all materials at room temperature (25 °C) before degassing corresponds exclusively to PF. In a normal oxygen-containing atmosphere the fluorescence intensity is also temperature independent. In order to study the HAE on the DF of C_{70} and of **1**, four solid solutions were prepared: C_{70} in PS,^[2] C_{70} in PBS, **1** in PS,^[2] and **1** in PBS. The effective concentration of bromide in PBS is 7.6 M. The films were prepared by evaporating a toluene solution of the corresponding fullerene and polymer which was previously deposited on a quartz plate. The films exhibit absorption spectra close to that of C_{70} and **1** in toluene, as shown in Figure 1 for C_{70} . These results are in agreement with a molecular dispersion of the fullerenes in the polymeric films.

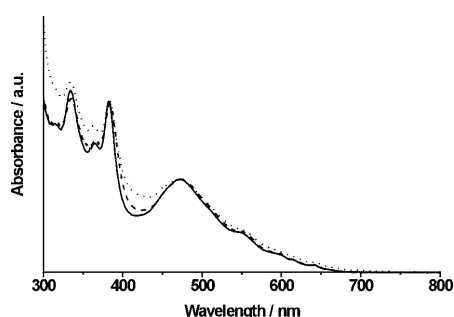


Figure 1. Absorption spectra of C_{70} in solution and in polymer films: toluene (—), PS (----) and PBS (.....).

The maximum absorption wavelength in the visible (460 nm) of **1** is also shorter than that of C_{70} (470 nm) (see Figure 2). The higher fluorescence quantum yield (9.4×10^{-4}) and fluorescence lifetime (0.85 ns) of **1**, when compared with

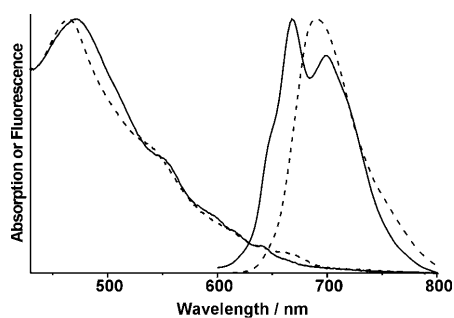


Figure 2. Absorption and fluorescence spectra of C_{70} -PS (—) and **1**-PS (----).

C_{70} (5.7×10^{-4} and 0.65 ns,^[22] respectively), both in toluene, and the fluorescence spectra with a single maximum (690 nm, see Figure 2) also correspond to the properties of a mono methano[70]fullerene.^[23] These changes are due to a minor reduction of the cage π -electronic system leading to an increase in the fluorescence lifetime and quantum yield.

The fluorescence spectra of the PS films are shown in Figure 2, and are similar to those in toluene. The presence of bromide in PBS polymer does not affect the fluorescence spectrum of C_{70} , showing the same maxima (670 and 700 nm) observed in PS. The derivative **1** displays the fluorescence maximum at 690 nm in PS as reported in toluene. However, the fluorescence maximum in PBS is red shifted to 700 nm.

The nonradiative decay rate constant controls the fluorescence decay of fullerenes, and is almost identical to the $S_1 \rightarrow T_1$ intersystem crossing rate constant. In this way, the measured lifetimes directly reflects the increased ISC rate constant by the HAE, when it exists. The fullerene lifetimes in the studied solid media are graphically summarized in Figure 3 and are also

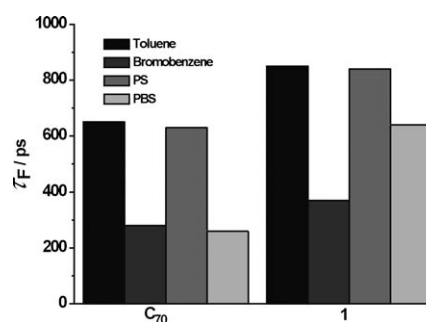


Figure 3. Comparison of the fluorescence lifetime of C_{70} and **1** in liquid solution and in polymer films.

given in Table 1. For the sake of comparison, lifetimes in toluene and bromobenzene are also given, and published values for a C_{70} pseudo-dihydro derivative^[2,24] are included as well. Several conclusions can be drawn: 1) The values obtained for

Table 1. Fluorescence lifetimes and fluorescence quantum yields.						
Compound	τ_F [ps]				$\Phi_F/10^{-4}$	
	MePh	PS	BrPh	PBS	MePh	BrPh
C_{70}	650 ^[15]	630 ^[2]	280 ^[15]	260	5.7 ^[15]	2.5 ^[15]
1	850	840	370	640	9.4	4.5
C_{70} dihydro ^[15]	1100	—	400	—	6.2	2.6

C_{70} and **1** in PS are identical to the values measured for the same compounds in toluene solution; 2) The lifetime of **1** decreases when bromobenzene is substituted for toluene, as observed in the cases of C_{70} and a C_{70} pseudo-dihydro derivative;^[2] 3) When comparing the data of the fluorescence lifetime of C_{70} in PS (0.63 ns) and PBS (0.26 ns), it is evident that the external HAE (in this case, a bromine atom in the polymer backbone) is responsible for the decrease in the fluorescence life-

time of C_{70} owing to the increase of the $S_1 \rightarrow T_1$ ISC; 4) The lifetime of C_{70} in bromobenzene is close to that in PBS, the effective concentration of bromine being relatively similar in both cases (7.6 M in PBS and 9.5 M in bromobenzene). 5) The heavy-atom effect in the solid state is less pronounced in **1**, with the lifetime in PBS (0.64 ns) being significantly higher than the value obtained in bromobenzene (0.37 ns), but still lower than in PS (0.84 ns), which can be tentatively explained by a lower effective bromine concentration in the neighbourhood of **1**, which is less soluble in PBS, and thus prone to preferential solvation. No evidence for solute aggregation was nevertheless found, as formation of C_{70} aggregates is known to lead to major changes in the absorption spectrum,^[25] and to strong fluorescence quenching and lifetime reduction.^[25]

The heavy-atom effect is also responsible for the decrease in the fluorescence quantum yields. Table 1 summarizes the fluorescence quantum yields of C_{70} , **1** and a C_{70} pseudo-dihydro derivative in toluene and bromobenzene. The decrease in the quantum yields of C_{70} and C_{70} pseudo-dihydro derivative when a brominated solvent is used is also observed for **1**. A significant decrease (more than 50%) in the fluorescence quantum yield of **1** is obtained when going from toluene to bromobenzene.

2.3. Delayed Fluorescence Intensity

The delayed fluorescence is only observable when oxygen is removed and as a consequence, quenching of the triplet state by this molecule is prevented. For this purpose, the samples were degassed and sealed, and afterwards fluorescence spectra were recorded for several temperatures. At room temperature, a significant enhancement of the fluorescence is observed in all cases (22-fold in the case of C_{70} -PS, 18-fold in C_{70} -PBS and four-fold for **1**-PS and **1**-PBS). This enhancement is a result of the additional contribution of DF to the total emission. Selected values of I_{DF}/I_{PF} for the fullerene-polymer films at different temperatures are given in Table 2.

Table 2. I_{DF}/I_{PF} values for the fullerene-polymer systems for selected temperatures.				
System (λ_{em})	25 °C	50 °C	70 °C	90 °C
C_{70} -PS ^[2] (700 nm)	22	39	53	64
C_{70} -PBS (700 nm)	18	34	53	66
1 -PS ^[2] (690 nm)	4	8	12	16
1 -PBS (700 nm)	4	8	13	17

The films were heated to a maximum of 90 °C, showing different levels of temperature dependence. After the heating measurements, a cooling half-cycle was performed. The fullerene-polymers films exhibit full reversibility and fluorescence is recovered without hysteresis, with a high level of reproducibility. The experimental and fitted values of I_{DF}/I_{PF} as a function of the temperature, Equation (18), are presented in Figure 4.

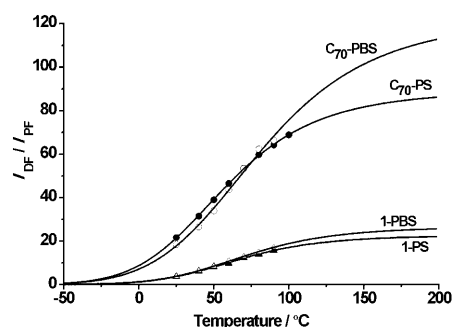


Figure 4. I_{DF}/I_{PF} vs temperature: Experimental points and calculated dependence (—), for C_{70} -PS (●), C_{70} -PBS (○), **1**-PS (▲) and **1**-PBS (△).

From Figure 4 it is possible to observe that the fit is quite good in all cases. The fluorescence of C_{70} in PS and in PBS significantly increases with temperature, which is a characteristic of DF. The same is observed for **1**, but to a smaller extent. In PS, the I_{DF}/I_{PF} ratio for **1** is on the average 4.5 times lower than that of C_{70} . Although the maximum experimental temperature was 90 °C, it is in principle possible to go to higher temperatures and further increase the I_{DF}/I_{PF} ratio (as the extrapolations in Figure 4 suggest). The fitted parameters Φ_T , ΔE_{ST} and Φ_S^∞ , along with Φ_F^{\max} , are given in Table 3. As can be seen, sensitivity to Φ_T is very high.^[2,4]

Table 3. Photophysical parameters obtained from steady-state data.					
System	Φ_T	ΔE_{ST} [kJ mol ⁻¹]	Φ_F^{\max} [%]	$-\log(\Phi_S^\infty)/10^{-7}$	$\tau_{DF}^{[a]}$ [ms]
C_{70} -PS	0.989	29	5	1.288	21
C_{70} -PBS	0.991	29	3	1.704	9
1 -PS	0.958	34	2	11.24	8
1 -PBS	0.963	34	2	11.27	7

[a] at 25 °C.

Using the method described above, a rounded value of 0.99 for the Φ_T of C_{70} is obtained in both PS and PBS. Nevertheless, a slight but significant increase is noticeable when going from PS to PBS. The same is observed for **1**, the rounded quantum yield of triplet formation being in this case 0.96. The fact that a nearly common Φ_T is measured for both polymers may appear to be in contradiction with the observed increase of the $S_1 \rightarrow T_1$ ISC rate constant when going from PS to PBS. However, this decay channel already overwhelmingly predominates, and therefore the effect of a further increase on a Φ_T which is already very close to one is quite small.

The computed temperature dependence of the fluorescence quantum yields of C_{70} and **1** is shown in Figure 5. It is seen that for both fullerenes the yields are always lower in PBS.

2.4. Delayed Fluorescence Lifetime

The delayed fluorescence lifetimes (τ_{DF}) of the degassed films are shown in Figure 6 as a function of temperature. As expected, they decrease with the increase of temperature, due to the

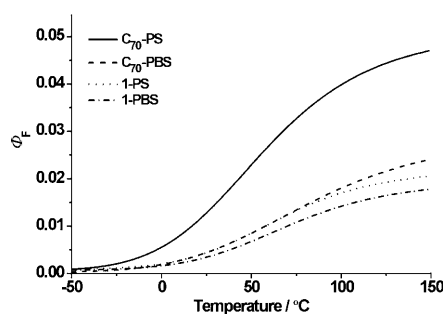


Figure 5. Computed fluorescence quantum yields vs temperature, for C_{70} -PS, C_{70} -PBS, 1-PS and 1-PBS.

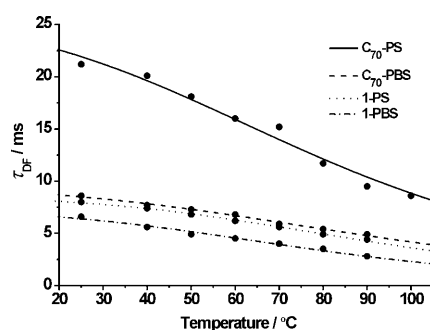


Figure 6. Temperature dependence of the experimental (●) and calculated delayed fluorescence lifetimes (τ_{DF}) of C_{70} -PS, C_{70} -PBS, 1-PS and 1-PBS.

increase of the $S_1 \leftarrow T_1$ rate constant. A general decrease of the delayed fluorescence lifetime when going from PS to PBS is observed. The room temperature values obtained for C_{70} , Table 3, are much lower in PBS (9 ms) than in PS (21 ms). In the case of 1 the decrease when going from PS (8 ms) to PBS (7 ms) is less marked.

Combining steady-state (intensity) and time-resolved (delayed fluorescence lifetimes) data according to Equation (22), good straight lines are obtained, see Figures 7 and 8. The recovered Φ_T coincide within experimental error with those previously determined solely on the basis of steady-state data. The τ_p^0 values are collected in Table 4 along with the A values, computed from Equation (17). The decrease in τ_p^0 results

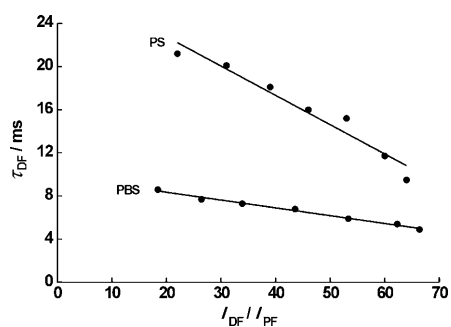


Figure 7. Plot according to Equation (22) of the experimental (●) and calculated (—) fluorescence data of C_{70} -PS and C_{70} -PBS.

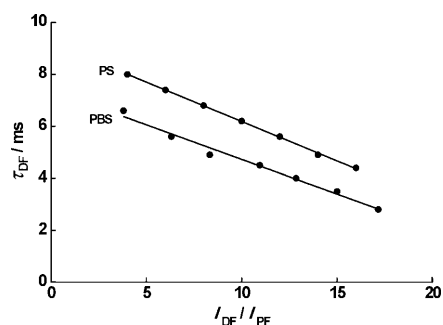
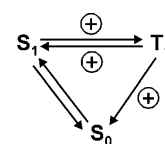


Figure 8. Plot according to Equation (22) of the experimental (●) and calculated (—) fluorescence data of 1-PS and 1-PBS.

Table 4. Photophysical parameters obtained from steady-state and time-resolved data.		
	$A/10^8 [s^{-1}]$	$\tau_p^0 [ms]$
C_{70} -PS	1.2	28
C_{70} -PBS	2.6	9.8
1-PS	4.2	9.2
1-PBS	5.2	7.4

mainly from an increase of the radiative rate constant owing to the HAE, as mentioned above.

The A pre-exponential factors increase when going from PS to PBS. As far as the authors are aware, this is the first experimental evidence for a HAE on the $S_1 \leftarrow T_1$ process. This was nevertheless expected on the basis of the principle of microscopic reversibility, as the HAE was observed to affect the $S_1 \rightarrow T_1$ ISC rate, see Table 1. Indeed, the ratio of the prompt fluorescence lifetimes in the two polymers is very close to the ratio of the A factors for both fullerenes (2.4 and 2.2 for C_{70} , and 1.3 and 1.2 for 1). In this way, the HAE increases all three rates: $S_1 \rightarrow T_1$, $S_1 \leftarrow T_1$, and $T_1 \rightarrow S_0$. The increase is more pronounced for C_{70} than for 1, which is probably related to a lower effective bromine concentration in the last case, as already mentioned. The HAE can be graphically summarized with reference to Scheme 1 as shown in Scheme 3.



Scheme 3. Influence of the HAE on the elementary photophysical processes.

The insensitivity of fluorescence intensities (I_{DF}/I_{PF}) to HAE can be explained by a cancellation of effects [see Eqs. (12) and (13)]: The increase of the $S_1 \rightarrow T_1$ and $S_1 \leftarrow T_1$ ISC rates, which by themselves increase the relative DF intensity, is nearly compensated by the concomitant increase of the $T_1 \rightarrow S_0$ radiative rate, which decreases the relative DF intensity. This is shown graphically for C_{70} in Figure 9, where the separate influence each process on the relative delayed fluorescence intensity is displayed. Similar results are obtained for 1.

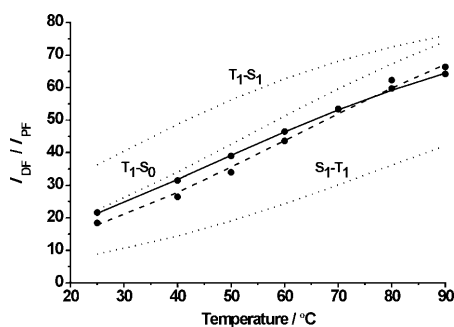


Figure 9. Separate and combined effects of photophysical processes on the relative delayed fluorescence intensity. The effect of $S_1 \rightarrow T_1$, $T_1 \rightarrow S_1$ and $T_1 \rightarrow S_0$ rate changes owing to the HAE is shown (.....). Experimental points (●) and calculated dependence from the combined effect of all three changes are also shown for C_{70} -PS (—) and C_{70} -PBS (-----).

3. Conclusions

The influence of the external heavy-atom effect (HAE) on the fluorescence properties of C_{70} and a C_{70} methano monoadduct was determined. In the absence of HAE (PS matrix) both fullerenes display a strong delayed fluorescence (DF) that is more pronounced in the case of C_{70} . In the presence of HAE (PBS matrix) the fluorescence intensities and delayed fluorescence lifetimes decrease significantly, whereas the relative delayed fluorescence intensities for each fullerene are surprisingly similar to the respective ones in PS for the full experimental temperature range. From the time and temperature dependence of fluorescence, a significant increase of the $S_1 \rightarrow T_1$, $S_1 \leftarrow T_1$, and $T_1 \rightarrow S_0$ conversion rates owing to the HAE is established. The external heavy-atom effect on a $S_1 \leftarrow T_1$ intersystem crossing rate is in particular reported here for the first time. The overall substantial insensitivity of relative DF intensities to HAE is explained by a compensation effect: As the $S_1 \rightarrow T_1$ and $S_1 \leftarrow T_1$ ISC rates on the one hand, and the $T_1 \rightarrow S_0$ radiative rate on the other hand work in opposition with respect to DF, a near cancellation of effects occurs.

Experimental Section

Materials: C_{70} (99%), polystyrene (PS, average $M_w \sim 280\,000$, pellets) and poly(4-bromostyrene) (PBS, average $M_w \sim 65\,000$, 43% Br, powder) were purchased from Aldrich (www.sigmaaldrich.com) and used as received. Toluene (MePh, Fluka, www.sigmaaldrich.com) and bromobenzene (BrPh, Fluka, www.sigmaaldrich.com) were of spectroscopic grade. C_{70} derivative **1** was synthesized as described in Supporting Information.

Preparation of the Films: To prepare the fullerene-containing films, C_{70} or **1** (2.37 mmol) and polymer (200 mg) were dissolved in toluene (1.8 mL), and the mixture was coated onto a quartz plate at room temperature. The plate was introduced into a quartz cell and degassed at room temperature with a turbomolecular pump (final pressure: ca. 3×10^{-8} atm), and the respective cell sealed afterwards.

Spectral Characterization: Absorption spectra of fullerenes in polymers films and in toluene were recorded on a UV-3101PC UV/Vis-NIR spectrophotometer (Shimadzu, www.shimadzu.com). The fluorescence quantum yields were determined from instrument-cor-

rected spectra using C_{70} in toluene as standard ($\Phi_F = 5.7 \times 10^{-4}$).^[26] Luminescence spectra were obtained with a Fluorolog F112 A fluorimeter (Spex, www.jobinyvon.com) in a front face configuration. Excitation wavelength was 470 nm, and the excitation and emission slits were 18 and 9 nm, respectively. The sample film was mounted slightly away from a 45° angle in order to minimize specular reflection of excitation light. Emission spectra were not corrected for the spectral response of the optics and photomultiplier. Temperature was controlled to within $\pm 0.5^\circ\text{C}$. Time-resolved picosecond fluorescence intensity decays were obtained by the single-photon timing method with laser excitation, with excitation at 470 nm and emission at 700 nm. The set-up consisted of a mode-locked Innova 400-10 argon-ion laser (Coherent, www.cohr.com) that synchronously pumped a cavity dumped 701-2 dye laser (Coherent, www.cohr.com), delivering 3–4 ps pulses (with ca. 40 nJ pulse^{-1}) at a frequency of 3.4 MHz. Intensity decay measurements were made by alternated collection of impulse and decays with the emission polarizer set at the magic angle position. Impulses were recorded slightly away from excitation wavelength with a scattering suspension. For the decays, a cut-off filter was used to effectively remove excitation light. Detection was always performed by passing the emission through a depolarizer and then through a HR320 monochromator (Jobin-Yvon, www.jobinyvon.com) with a grating of $100 \text{ lines mm}^{-1}$. Usually no less than 5000 counts were accumulated at the maximum channel. A 2809U-01 microchannel plate photomultiplier (Hamamatsu, www.hamamatsu.com) served as the detector. Its response function had an effective FWHM of 35 ps.^[27]

Acknowledgements

This work was supported by Fundação para a Ciência e a Tecnologia (FCT, Portugal) and POCI 2010 (FEDER) within project PTDC/ENR/64909/2006.

Keywords: [70]fullerene · delayed fluorescence · fluorescence spectroscopy · fullerenes · heavy-atom effect

- [1] B. Valeur, *Molecular Fluorescence: Principles and Applications*, Wiley-VCH, Weinheim, 2002.
- [2] C. Baleizão, M. N. Berberan-Santos, *J. Chem. Phys.* **2007**, *126*, 204510.
- [3] C. Baleizão, M. N. Berberan-Santos, *ChemPhysChem* **2009**, *10*, 199–205.
- [4] M. N. Berberan-Santos, J. M. M. Garcia, *J. Am. Chem. Soc.* **1996**, *118*, 9391–9394.
- [5] S. M. Bachilo, A. F. Benedetto, R. B. Weisman, J. R. Nossal, W. E. Billups, *J. Phys. Chem. A* **2000**, *104*, 11265–11269.
- [6] F. A. Salazar, A. Fedorov, M. N. Berberan-Santos, *Chem. Phys. Lett.* **1997**, *271*, 361–366.
- [7] B. Gigante, C. Santos, T. Fonseca, M. J. M. Curto, H. Luftmann, K. Bergander, M. N. Berberan-Santos, *Tetrahedron* **1999**, *55*, 6175–6182.
- [8] S. M. Anthony, S. M. Bachilo, R. B. Weisman, *J. Phys. Chem. A* **2003**, *107*, 10674–10679.
- [9] C. Baleizão, S. Nagl, S. Borisov, M. Schäferling, O. S. Wolfbeis, M. N. Berberan-Santos, *Chem. Eur. J.* **2007**, *13*, 3643–3651.
- [10] V. Augusto, C. Baleizão, M. N. Berberan-Santos, J. P. Farinha, *J. Mater. Chem.* **2010**, *20*, 1192–1197.
- [11] S. Nagl, C. Baleizão, S. M. Borisov, M. Schäferling, M. N. Berberan-Santos, O. S. Wolfbeis, *Angew. Chem.* **2007**, *119*, 2368–2371; *Angew. Chem. Int. Ed.* **2007**, *46*, 2317–2319.
- [12] C. Baleizão, S. Nagl, M. Schäferling, M. N. Berberan-Santos, O. S. Wolfbeis, *Anal. Chem.* **2008**, *80*, 6449–6457.
- [13] J. B. Birks, *Photophysics of Aromatic Molecules*, Wiley, London, 1970.
- [14] Y. Zeng, L. Biczok, H. Linschitz, *J. Phys. Chem.* **1992**, *96*, 5237–5239.

- [15] S. Foley, M. N. Berberan-Santos, A. Fedorov, R. Bensasson, S. Leach, B. Gigante, *Chem. Phys.* **2001**, *263*, 437–447.
- [16] I. Texier, M. N. Berberan-Santos, A. Fedorov, M. Brettreich, H. Schonberger, A. Hirsch, S. Leach, R. V. Bensasson, *J. Phys. Chem. A* **2001**, *105*, 10278–10285.
- [17] M. Rae, A. Fedorov, M. N. Berberan-Santos, *J. Chem. Phys.* **2003**, *119*, 2223–2231.
- [18] M. Rae, F. Perez-Balderas, C. Baleizão, A. Fedorov, J. A. S. Cavaleiro, A. C. Tomé, M. N. Berberan-Santos, *J. Phys. Chem. B* **2006**, *110*, 12809–12814.
- [19] E. N. Bodunov, M. N. Berberan-Santos, *Chem. Phys.* **2004**, *301*, 9–14.
- [20] W. E. Graves, R. H. Hofeldt, S. P. McGlynn, *J. Chem. Phys.* **1972**, *56*, 1309–1314.
- [21] C. A. Parker, *Photoluminescence of Solutions*, Elsevier, Amsterdam, **1968**.
- [22] A. Fedorov, M. N. Berberan-Santos, J.-P. Lefèvre, B. Valeur, *Chem. Phys. Lett.* **1997**, *267*, 467–471.
- [23] M. J. Brites, C. Santos, S. Nascimento, B. Gigante, H. Luftmann, A. Fedorov, M. N. Berberan-Santos, *New J. Chem.* **2006**, *30*, 1036–1045.
- [24] S. Foley, M. N. Berberan-Santos, A. Fedorov, D. J. McGarvey, C. Santos, B. Gigante, *J. Phys. Chem. A* **1999**, *103*, 8173–8178.
- [25] H. N. Ghosh, A. V. Sapre, J. P. Mittal, *J. Phys. Chem.* **1996**, *100*, 9439–9443.
- [26] B. Ma, Y.-P. Sun, *J. Chem. Soc. Perkin Trans. 2* **1996**, 2157–2162.
- [27] A. A. Fedorov, S. P. Barbosa, M. N. Berberan-Santos, *Chem. Phys. Lett.* **2006**, *421*, 157–160.

Received: May 19, 2010

Revised: June 25, 2010

Published online on August 18, 2010